

Instability development of a viscous liquid drop impacting a smooth substrate

Lei Xu (徐磊)

Department of Physics, The Chinese University of Hong Kong, Hong Kong, People's Republic of China

(Received 13 July 2010; published 30 August 2010)

We study the instability development during a viscous liquid drop impacting a smooth substrate, using high-speed photography. The onset time of the instability highly depends on the surrounding air pressure and the liquid viscosity: it decreases with air pressure with the power of minus two, and increases linearly with the liquid viscosity. From the real-time dynamics measurements, we construct a model which compares the destabilizing stress from air with the stabilizing stress from liquid viscosity. Under this model, our experimental results indicate that at the instability onset time, the two stresses balance each other. This model also illustrates the different mechanisms for the inviscid and viscous regimes previously observed: the inviscid regime is stabilized by the surface tension and the viscous regime is stabilized by the liquid viscosity.

DOI: [10.1103/PhysRevE.82.025303](https://doi.org/10.1103/PhysRevE.82.025303)

PACS number(s): 47.20.Ma, 47.55.Ca, 47.55.dr

The phenomenon of a liquid drop hitting a solid surface is ubiquitous: it occurs whenever the very first rain drop reaches the ground or when we spill coffee onto the floor. Liquid-solid impact has been extensively studied due to its broad applications in many industrial processes, such as ink-jet printing, surface coating, combustion of liquid fuel, plasma spraying, and pesticide application [1]. It may seem obvious that the impact outcomes should be determined by either the liquid or the solid properties [2–7], however, recent studies surprisingly revealed the crucial role of the surrounding atmosphere: reducing air pressure can completely suppress the liquid drop splashing on a smooth substrate [8,9], and the compressibility of the surrounding air is demonstrated to be important [10,11]. This unexpected discovery brings a completely new effect, the air effect, into the impact problem. To fully understand this new effect, therefore, it is essential to clarify the interactions between air and the fundamental liquid properties, such as surface tension and viscosity. Previous study has shown that the competition between the air effect and the liquid surface tension determines the impact outcomes of inviscid liquid drops [8]. However, there has been very limited study on the interaction between air and the liquid viscosity, although the liquid viscosity itself has been broadly tested [2,3,12] and the entrapment of air bubbles in viscous drops was illustrated recently [13,14]. As a result, the relationship between surrounding air and the liquid viscosity is still missing, and the understanding on the liquid-solid impacts, especially the newly discovered air effect, remains incomplete.

In this paper, we systematically study the interaction between air and the liquid viscosity by varying both the surrounding air pressure and the liquid viscosity, for the impacts of viscous liquid drops on a smooth substrate. With high-speed photography, we find that the instability produced by an impact highly depends on the air pressure and the liquid viscosity: the onset time of the instability decreases with air pressure with the power law of minus two, while it increases linearly with the liquid viscosity. From the real-time liquid motion measurements, we construct a simple model that compares the destabilizing stress from air with the stabilizing stress from the liquid viscous stress. The experimental results support the picture that the two stresses balance each other at

the instability onset time. This model also predicts the existence of a threshold viscosity, above which the system is stabilized by the liquid viscosity, and below which it is stabilized by the surface tension. This prediction quantitatively agrees with the previous experiment [9].

We perform all the experiments inside a transparent vacuum chamber whose pressure can be continuously varied from 1 to 102kPa (atmospheric pressure). We also independently vary the liquid viscosity by using silicone oils of very close densities ($0.92\sim 0.94\text{ g cm}^{-3}$) and surface tensions ($19.7\sim 20.5\text{ mN m}^{-1}$) but different dynamic viscosities ($4.65\sim 13.2\text{ mPa s}$). We note that all our liquids wet the substrate completely thus the wetting conditions are kept the same for all the impacts. To make sure that identical impact conditions are achieved each time, we release reproducible liquid drops of diameter $d=3.1\pm 0.1\text{ mm}$ from a fixed height, and all the liquid drops impact a smooth and dry glass substrate at the velocity $V_0=4.03\pm 0.05\text{ m s}^{-1}$. The impacts are subsequently recorded by a high-speed camera at the frame rate of 47 000 frames per second.

We probe the air-liquid interaction by inspecting the instability development during the impact: under high-speed photography, the impact produces a thin liquid film expanding radially along the substrate. This liquid film is stable initially, however, a small rim shows up around the edge at a certain moment, and subsequently develops into larger and larger undulations (see Fig. 1 left column). We believe the appearance of the rim indicates the transition from a stable system into an unstable one, and define the moment of the rim appearance as the instability onset time, t_{on} . For example, an instant very close to t_{on} is shown in the third image of Fig. 1 left column. This instability onset time, t_{on} , measures how fast the system goes unstable: the smaller it is, the faster the system becomes unstable. Interestingly, t_{on} has a strong dependence on the surrounding air pressure, P . The two columns in Fig. 1 show two almost identical impacts, with only different P : At $P=40\text{ kPa}$ (left column), instabilities show up in the third image; while at a higher pressure, $P=63\text{ kPa}$ (right column), they appear at a much earlier time in the second image.

By performing similar experiments under different air pressures, we systematically measure the instability onset

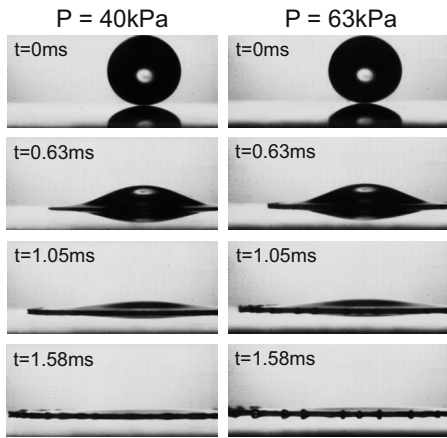


FIG. 1. Instability development under different pressures. The liquid drop has diameter $d=3.1 \pm 0.1$ mm, dynamic viscosity $\mu=6.71 \pm 0.02$ mPa s, and impact velocity $V_0=4.03 \pm 0.05$ m s $^{-1}$. The left column shows an impact under the air pressure $P=40$ kPa. The impact is initially stable, but instability shows up from the third image. The right column shows an identical impact under higher pressure, $P=63$ kPa. The instability appears at a much earlier time from the second image.

time, t_{on} , with respect to the pressure, P . We find that t_{on} decreases monotonically with P , as shown in Fig. 2. Intuitively, this implies that more air leads to earlier instability appearance, thus air acts to destabilize the system, consistent with previous findings [8]. To test the interaction between air pressure and liquid viscosity, we perform the same t_{on} vs P measurements with silicone oils of very similar mass density and surface tension, but different dynamic viscosities, as plotted by the different symbols in Fig. 2. From bottom to top, the four curves correspond to increasing dynamic viscosities: $\mu=4.65$ (●), 6.7 (○), 9.3(▲), and 13.2 (×) mPa s. Intriguingly, all the data can be excellently fitted by a simple functional form: $t_{on}=A/P^2+t_0$, with A and t_0 the fitting pa-

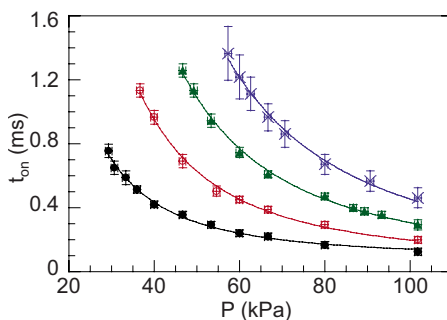


FIG. 2. (Color online) The instability onset time, t_{on} , vs P for liquids of different viscosities. From bottom to top, the four curves correspond to increasing viscosities: $\mu=4.65$ (●), 6.7 (○), 9.3(▲), and 13.2 (×) mPa s. All the curves can be fitted by a universal functional form: $t_{on}=A/P^2+t_0$. t_0 ranges from 0.03 to 0.09 ms, much smaller than most t_{on} values. The prefactor A increases with μ , as demonstrated by the higher locations of the liquids with larger μ . Limited by the experimental condition, each data set has only about one decade in x and y directions. But it is nonetheless impressive that one simple functional form can fit all the data sets well.

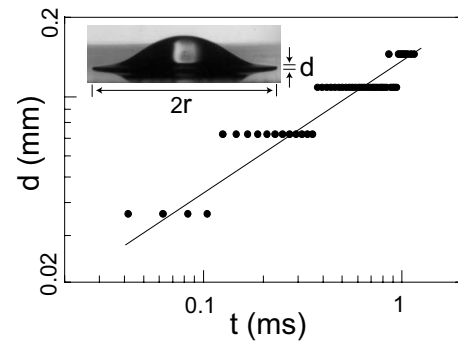


FIG. 3. Direct measurement of the thickness d vs time t . The impact is by a liquid drop of $\mu=4.65$ mPa s and $V_0=4.03 \pm 0.01$ m/s. The inset shows a typical snapshot from which d is measured: d is the liquid film thickness measured at the edge. Main panel shows the measured $d(t)$. Because d is quite small, the four discrete values correspond to one, two, three, and four pixels of our camera. The fit is: $d=1.9\sqrt{vt}$, indicating that d is determined by the boundary layer thickness: \sqrt{vt} .

rameters. t_0 has typical values between 0.03 and 0.09ms, much smaller than most t_{on} values. However, it is still larger than our time resolution (0.02 ms) and cannot be explained as measurement errors. One possibility is that the system actually becomes unstable slightly earlier than the measured t_{on} , but the instability features at that moment are too tiny to visualize. The prefactor, A , increases with the viscosity, μ , as illustrated by the higher locations for larger viscosity liquids. This result can be intuitively understood: the larger the viscosity, the more stable the system is, and the later the instability shows up. Limited by experimental conditions, each data set only has the dynamic range of about one decade in time and pressure, but it is nevertheless impressive that one simple functional form fits all the curves nicely.

Together these data demonstrate that the instability development depends on both P and μ , but they play opposite roles: P acts to destabilize the interface since higher P leads to faster growth of the instability; while μ favors stabilizing the interface as higher μ slows down the instability growth. To quantitatively understand the effects of P and μ , we inspect their corresponding stresses: at the edge of the expanding liquid film, air pressure applies a destabilizing stress, $\Sigma_G \sim \rho_G C_G V_e$ [8]; and the liquid viscosity produces a stabilizing stress, $\Sigma_\mu \sim \mu V_e / d$. Here ρ_G is the density of the surrounding gas, C_G is the speed of the sound in the gas, V_e is the liquid disk expanding velocity, and d is the liquid film thickness measured at the edge. C_G enters the problem because previous experiments [8,9] and simulations [10,11] suggest that the compressibility of the surrounding air is important.

Since V_e and d vary with time, so do Σ_G and Σ_μ . Therefore a careful examination on their time dependence could provide valuable insight for the instability development. We can directly measure $r(t)$ and $d(t)$ from high-speed photography, as illustrated in Fig. 3 upper inset. V_e can be obtained by taking the time derivative of $r(t)$. Our measurements show that $r(t) \propto \sqrt{t}$, consistent with previous studies, thus $V_e = dr/dt \propto 1/\sqrt{t}$. This time dependence keeps valid for most of the expanding period, within which all our measurements

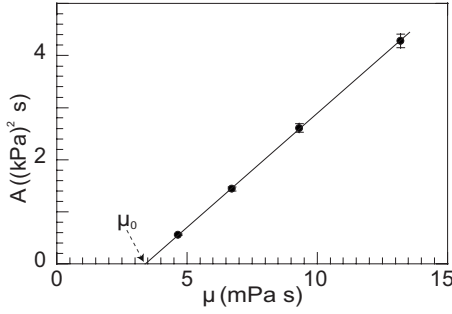


FIG. 4. The prefactor, A , vs liquid viscosity, μ , for the curves shown in Fig. 2. The prefactors are obtained from the best fits in Fig. 2. A varies linearly with μ and intercepts the x axis at $\mu_0 = 3.4$ mPa S. μ_0 agrees with the threshold viscosity separating the inviscid and viscous regimes observed in previous experiment [9].

are performed. Moreover, we can directly measure the thickness of the liquid film, d , with respect to t , as plotted in the main panel of Fig. 3. Because the small values of d approach the single pixel level of our camera, the data are quite discrete; nonetheless they are consistent with the fit: $d \sim \sqrt{\nu t}$, with $\nu = \mu/\rho_L$ being the liquid kinematic viscosity. This shows that d is determined by the boundary layer thickness, $\sqrt{\nu t}$.

From the real-time dynamics, we derive the time dependence of the stresses: The destabilizing stress, $\Sigma_G \sim \rho_G C_G V_e \propto 1/\sqrt{t}$, decreases with t with the power of $-\frac{1}{2}$; while the stabilizing stress, $\Sigma_\mu \sim \mu V_e/d \propto 1/t$, depends on t with the power of -1 . Clearly, when t is small, $\Sigma_\mu \gg \Sigma_G$, and the stabilizing stress dominates the destabilizing stress. This implies that the system should be stable initially, as we have observed. As t increases, however, Σ_μ decreases much faster than Σ_G and a crossover should occur at a certain time. After this crossover time, Σ_G becomes dominant and the system will go unstable. The experiments are consistent with this picture: all the impacts are indeed stable initially and become unstable after the instability onset time, t_{on} . Therefore t_{on} naturally corresponds to the crossover time at which the two stresses balance each other,

$$\rho_G C_G V_e \sim \mu \frac{V_e}{d} \Big|_{t=t_{on}}. \quad (1)$$

Plugging in the relations: $\rho_G \propto P$ and $d \propto \sqrt{\mu t}$, with V_e canceling each other on both sides and C_G being a constant independent of P , we reach the expression,

$$t_{on} \propto \frac{\mu}{P^2}. \quad (2)$$

This expression successfully explains the two main features observed in Fig. 2: (1) $t_{on} - t_0 \propto 1/P^2$ and (2) the prefactor of this dependence, A , increases with μ . Moreover, Eq. (2) further predicts that A should increase linearly with μ . To test this prediction, we find A for each viscosity in Fig. 2 from the best fit (the solid curves in Fig. 2), and plot A as the function of μ in Fig. 4. Indeed, a very nice linear dependence is observed but the line does not go through the origin; in-

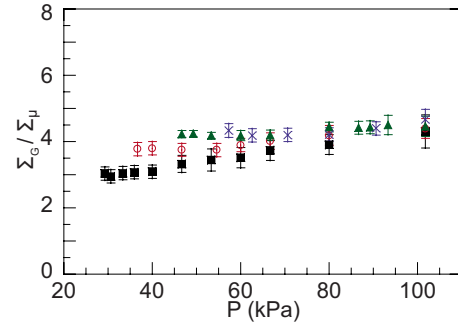


FIG. 5. (Color online) The ratio between the destabilizing and the stabilizing stresses, Σ_G/Σ_μ , measured at $t=t_{on}$, for various pressures and viscosities. All experiments are done under almost identical impact conditions, with only the pressure being varied. Different symbols represent liquids of different viscosities: $\mu = 4.65$ (●), 6.7 (○), 9.3 (▲), and 13.2 (×) mPa s. The ratio, $\Sigma_G/\Sigma_\mu \sim \rho_G C_G d/\mu$, is computed from direct measurements: ρ_G is calculated from P , and d is from the best fit to the high-speed images at the time t_{on} . Without any fitting parameter, all the ratios are within the narrow range between 3 and 4, confirming that Σ_G and Σ_μ are comparable at the time t_{on} .

stead, it intercepts the x axis at the finite viscosity value, $\mu_0 = 3.4$ mPa s.

What is the physical meaning of μ_0 ? To answer this question, we need to understand the impacts by the inviscid liquids with $\mu < \mu_0$. Previous study showed that for an inviscid liquid drop impacting on a smooth surface, the destabilizing stress is the same as the current viscous case, $\Sigma_G \sim \rho_G C_G V_e$ [8]. However, the stabilizing stress, Σ_L , is quite different. Σ_L comes from the liquid surface tension, and is typically estimated as the surface tension coefficient, σ , divided by the liquid film thickness, d : $\Sigma_L \sim \sigma/d$ [8]. Therefore, we propose that the complete stabilizing effect for an impact should include both the surface tension component, Σ_L , and the viscosity component, Σ_μ . When the viscosity is small, Σ_L dominates Σ_μ , and we get typical inviscid behavior [15]. However, when μ exceeds a certain threshold value, the viscous stress Σ_μ will become the major stabilizing factor, and we get the currently observed viscous behavior. Therefore μ_0 naturally corresponds to this threshold viscosity which determines whether the inviscid or the viscous model should be used. We note that μ_0 should depend on detailed impact conditions such as the impact velocity, surface tension and wetting conditions. Previous experiments with similar impact conditions already confirmed that two impact regimes exist when μ is varied, and the transition from the inviscid regime to the viscous regime is close to μ_0 (see Ref. [9], Fig. 5). This provides strong experimental evidence for the physical meaning of μ_0 . Moreover, our picture not only explains the meaning of μ_0 , it also demonstrates the main difference between the two impact regimes: the inviscid regime is stabilized by the surface tension and the viscous regime is stabilized by the liquid viscosity.

We propose that in the viscous regime, the stabilizing stress is mainly from the viscous stress, $\Sigma_\mu \sim \mu V_e/d$, and construct a model which compares Σ_μ with the destabilizing stress, $\Sigma_G \sim \rho_G C_G V_e$. By assuming that Σ_G and Σ_μ balance each other at the instability onset time, t_{on} [Eq. (1)], we suc-

cessfully explain the dependence of t_{on} on P and μ : $t_{on} - t_0 = A/P^2$ and $A \propto \mu - \mu_0$, with μ_0 the threshold viscosity separating the inviscid and the viscous regimes. However, the most critical criterion, whether Σ_G and Σ_μ are indeed comparable at t_{on} , remains to be verified. To test it quantitatively, we measure the ratio between the two stresses, $\Sigma_G/\Sigma_\mu \sim \rho_G C_G d/\mu$, at the moment t_{on} . This ratio is tested for various pressures and viscosities, as plotted in Fig. 5. All experiments are done under almost identical impact conditions, with only the pressure being varied. Different symbols represent liquids of different viscosities: $\mu=4.65$ (●), 6.7 (○), 9.3 (▲), and 13.2 (×) mPa s. For each impact, we obtain d value at t_{on} from the high-speed photography measurements [16]. The air density ρ_G is directly computed from the pressure P . The speed of sound in air at room temperature (20 °C), $C_G=343$ m s⁻¹, is a constant independent of P . Plugging in all the values, we obtain the ratio, Σ_G/Σ_μ , as plotted in Fig. 5. Without any fitting parameter, most data points collapse to the narrow range between 3 and 4. These values prove that Σ_G and Σ_μ are indeed comparable at the time t_{on} , as our model predicts.

We study the interaction between the air pressure and the liquid viscosity for the impact of a liquid drop on a smooth substrate. For viscous liquids, the impact is stabilized by the viscous stress, $\Sigma_\mu \sim \mu V_e/d$, whose competition with the de-

stabilizing stress determines when the system becomes unstable. By contrast, for inviscid liquids, the stabilizing stress comes from the surface tension, $\Sigma_L \sim \sigma/d$. Interestingly, by inspecting the two different stabilizing stresses, we find that the liquid viscosity plays opposite roles in them. For Σ_L in the inviscid regime, we have $\Sigma_L \sim \sigma/d \sim \sigma/\sqrt{vt} \propto 1/\sqrt{\mu}$. Here larger μ leads to larger d and smaller Σ_L , thus more viscous liquids are less stable. However, in the viscous regime, we have $\Sigma_\mu \sim \mu V_e/d \propto \sqrt{\mu}$ [17]. Now increasing μ will increase Σ_μ and make the system more stable. This nonmonotonic behavior was already observed by previous experiments (see Ref. [9], Fig. 5) and now can be fully understood. In summary, our study shows that the interplay between air and liquid viscosity is crucial in determining the outcomes of liquid-solid impacts. The viscosity plays different roles in different regimes, and the simple intuition that a more viscous liquid is more stable during an impact is not always valid.

We gratefully acknowledge helpful discussions with Sidney Nagel, Wendy Zhang, Michelle Driscoll, Alexis Berges, and Emily Ching. This project is supported by RGC Research Grant Direct Allocation (Project No. 2060395), MR-SEC Grant No. DMR-0213745, and NSF Grant No. DMR-0352777.

-
- [1] A. L. Yarin, *Annu. Rev. Fluid Mech.* **38**, 159 (2006).
 [2] C. Mundo, M. Sommerfeld, and C. Tropea, *Int. J. Multiphase Flow* **21**, 151 (1995).
 [3] R. Rioboo, M. Marengo, and C. Tropea, *Atomization Sprays* **11**, 155 (2001).
 [4] D. Richard, C. Clanet, and D. Quéré, *Nature (London)* **417**, 811 (2002).
 [5] N. Z. Mehdizadeh, S. Chandra, and J. Mostaghimi, *J. Fluid Mech.* **510**, 353 (2004).
 [6] Tsai *et al.*, *Langmuir* **25**, 12293 (2009).
 [7] R. D. Deegan, P. Brunet, and J. Eggers, *Nonlinearity* **21**, C1 (2008).
 [8] L. Xu, W. W. Zhang, and S. R. Nagel, *Phys. Rev. Lett.* **94**, 184505 (2005).
 [9] L. Xu, *Phys. Rev. E* **75**, 056316 (2007).
 [10] S. Mandre, M. Mani, and M. P. Brenner, *Phys. Rev. Lett.* **102**, 134502 (2009).
 [11] M. Mani, S. Mandre, and M. P. Brenner, *J. Fluid Mech.* **647**, 163 (2010).
 [12] R. D. Schroll, C. Josserand, S. Zaleski, and W. W. Zhang, *Phys. Rev. Lett.* **104**, 034504 (2010).
 [13] S. T. Thoroddsen *et al.*, *J. Fluid Mech.* **545**, 203 (2005).
 [14] S. T. Thoroddsen, K. Takehara, and T. G. Etoh, *Phys. Fluids* **22**, 051701 (2010).
 [15] We note that $\Sigma_\mu \propto 1/t$ while $\Sigma_L \propto 1/d \propto 1/\sqrt{t}$. Thus Σ_μ always dominates for small t . However, Σ_μ decreases more rapidly with t and can drop below Σ_L soon after the impact, for the case of small μ . Therefore, Σ_L can be dominant for most period of the impact in the inviscid regime.
 [16] Due to the discreteness of the measured d values, we use the calculated d value at $t=t_{on}$ from the best fitting function such as the solid line shown in Fig. 3 lower inset.
 [17] Actually V_e also depends on μ . But the dependence is much weaker than $\sqrt{\mu}$ (unpublished data), and qualitatively our argument is not affected. We also note that in Eq. (1), V_e cancels out, thus its dependence on μ does not affect the derivation of Eq. (2).